Research Square

Preprints are preliminary reports that have not undergone peer review.
They should not be considered conclusive, used to inform clinical practice,
or referenced by the media as validated information.

Myocardial ischemia-reperfusion injury alters inflammation-associated gut microbiota

Cuifang Kuang
Jiangxi University of Traditional Chinese Medicine
Lingqin Su
Jiangxi University of Traditional Chinese Medicine
Manman Qin
Jiangxi University of Traditional Chinese Medicine
Liang Qiu (liangqiu@jxutcm.edu.cn)
Jiangxi University of Traditional Chinese Medicine https://orcid.org/0000-0001-5850-1455
Jun Yu
Temple University

Research

Keywords: Ischemia-reperfusion injury, Gut microbiota, Inflammation

Posted Date: January 30th, 2020

DOI: https://doi.org/10.21203/rs.2.22246/v1

License: This work is licensed under a Creative Commons Attribution 4.0 International License.
Read Full License

Abstract

Background

The gut microbiota plays important roles in the development of cardiovascular diseases. However, whether myocardial ischemia–reperfusion (I/R) alters gut microbiota composition and its significance remains unknown. In this work, Sprague–Dawley rats were subjected to left anterior descending coronary artery ligation and reperfusion. The fecal DNA isolated before myocardial ischemia and after reperfusion were analyzed for microbiota changes by high-throughput 16S rDNA sequencing.

Results

Results showed that compared with the pre-I/R and pre-sham surgery group, I/R and sham surgery significantly increased the relative abundance of the phyla *Proteobacteria* , and decreased the relative abundance of the phylum *Firmicutes* . The I/R surgical procedure increased the proportions of phylum *Spirochaetes* and genus *Enterococcus* compared to pre-I/R and sham surgery group. Moreover, I/R surgery significantly worsened the infiltration of macrophages into heart tissue compared with sham surgery.

Conclusions

Taken together, these findings suggested that myocardial I/R altered the gut microbiota profile, which may promote inflammatory cell infiltration in the injured heart.

Background

Cardiovascular and cerebrovascular ischemic diseases are leading causes of death in human. More than one million Americans suffer from myocardial infarction, stroke, and other thrombotic diseases each year [1]. Ischemia occurs when blood supply to a tissue is occluded. The restoration of blood flow after tissue ischemia increases both local and systemic inflammation response and results in the release of inflammatory mediators, such as IL-6, tumor necrosis factor-α, and IL-1β, leading to multiple organ failure and thus inducing significant morbidity and mortality [2, 3].

The gut microbiota was recently found to play important roles in the development of cardiovascular diseases [4–6], and a growing body of evidence shows a direct interaction between gut microbiota and the severity of ischemia–reperfusion (I/R) injury in multiple organs. Following mesenteric I/R, germ-free mice or mice treated with broad-spectrum antibiotics exhibited decreased intestine and lung injuries and systemic inflammation compared with conventional mice [7–9]. Moreover, the depletion of gut microbiota offers protection against renal I/R injuries, such as renal tissue damage, dysfunction, and remote organ injury [10]. In mice, treatment with antibiotics attenuates circulating and lung inflammatory markers after lung I/R [11]. Beneficial probiotics Clostridium butyricum weaken cerebral I/R injury in diabetic mice by altering the gut microbiota composition [12].

In addition to the direct evidence demonstrating that gut microbiota influences I/R injury, Toll-like receptor (TLR) family members, which recognize pathogen-associated molecular patterns [13], are involved in I/R-mediated tissue damage and inflammation [14, 15]. Dexmedetomidine, a neuroprotective agent, protects nerves from cerebral I/R injury by inactivating the TLR-4/NF-κB pathway [16], and TLR-4 deficiency prevents focal cerebral ischemia and axotomy-induced neurodegeneration [17]. TLR-2 and TLR-3, receptors of pathogen-associated molecular and double-stranded nucleotides, respectively, contribute to the pathogenesis of early acute kidney injury following renal I/R [18, 19]. The TLR/MyD88 pathway also promotes acute intestinal and lung injury, inflammation, and endothelial damage after intestinal I/R [20]. On the other hand, some studies express the opposite view in that the gut microbiota protects against I/R-induced intestinal injury [21, 22]. Therefore, the positive or negative relationships between gut microbiota alteration and I/R injury need to be further illustrated.

Myocardial I/R injury promotes adverse cardiovascular outcomes, including decreased systolic function; decreased coronary flow; and vascular reactivity changes after myocardial ischemia, and in some cases circulatory arrest [23]. It has been shown that the compositions of gut microbiota changes after acute myocardial infarction [24, 25]. In rats, vancomycin treatment alters the relative abundance of gut microbiota, decreases myocardial infarct size, and improves recovery of post-ischemic mechanical function [26, 27]. In addition, the expression level of TLR-4/NF-κB is positively correlate with myocardial I/R injury in mice [28]. Taken together, these studies suggest that the gut microbiota may be involved in I/R injury and systemic inflammation in mice.

In the present study, we adopted a rat model of myocardial I/R induced by left anterior descending (LAD) coronary artery occlusion and aimed to investigate whether myocardial I/R surgery directly influences gut microbiota composition. Moreover, by using next-generation sequencing method, we determined the types of gut microbiota associated with inflammation, and compared the changes in this microbiota after myocardial I/R surgery and sham operation.

Results

Characteristics of rat myocardial I/R model.

ST segment elevation is one of the most important electrocardiographic features after myocardial I/R injury [29]. To determine that the rat model of myocardial I/R was established, the ST segment and TTC staining of the hearts from the sham and I/R groups were evaluated. As seen in Fig. 1A, the ST segment of the I/R group was significantly elevated by 0.3769 mv compared to that of the sham group. In addition, TTC staining of the hearts showed infarct size (36.06% ± 3.76%) of the I/R group significantly increased in relative to that (3.76% ± 0.23%) of the sham group (Fig. 1B and 1C). These results suggested that the animal model of myocardial I/R was successfully established.

I/R induces myocardial inflammation and macrophage infiltration.

To evaluate whether inflammation was induced by myocardial I/R, we performed H&E staining, which revealed the remarkable infiltration of inflammatory cells in the hearts of the myocardial I/R-operated rats compared to that in the sham operated rats (Fig. 2A). Macrophage infiltration was further identified using immunohistochemical staining for CD68, a macrophage-specific marker. The results showed a significant increase in CD68-positive macrophages in the myocardial of I/R-operated rats compared with sham (Fig. 2B), suggesting I/R injury induced inflammatory cell infiltration in the heart.

Myocardial I/R injury alters the composition of gut microbiota in rat.

To study whether myocardial I/R injury will lead to gut microbiota alteration, we collected fecal samples from the sham and I/R groups before and after surgery. We subsequently performed 16S rRNA gene sequencing analysis using the Illumina MiSeq PE250 platform and obtained a total of 377034 paired-end reads with an average of 31419.5 reads per sample. The overlapping paired-end reads were merged to 374970 tags with a mean of 31247 tags. The clean tags were clustered in 871 OTUs with a mean of 457 OTUs per sample at 97% identity. The OTUs were annotated to microbial taxa. Rarefaction analysis (Figure S1A) tended to be asymptotic, Shannon–Wiener diversity index estimates were stable (Figure S1B), and Good's coverage index (99.74% ± 0.07%) indicated that the sequencing methodology was appropriate to evaluate the microbial diversity among the groups. Further analysis showed that I/R surgery significantly influenced the ACE, Chao1, Shannon's, Simpson's, and Good's coverage indices for gut bacteria compared with the sham group (Fig. 3). Overall, 11 identical phyla were identified in each of the sample. Within those, five phyla (Actinobacteria, Bacteroidetes, Firmicutes, Proteobacteria, and Spirochaetes) dominated the bacterial community, although their relative abundance varied in each sample (Table S1).

To directly exam the association between myocardial I/R injury and gut microbiota, we firstly analyzed the fecal samples obtained from pre- and post-I/R surgery. A Venn diagram of OTUs with 97% similarity was shown in Figure S2. There were 548 shared OTUs, and 80 and 177 unique OTUs in the post- and pre-I/R samples, respectively. PCoA analysis based on weighted and unweighted UniFrac distances revealed distinct clusters in the pre- and post-I/R surgery groups, suggesting that I/R induced significant changes in the overall cecal microbial composition (Fig. 4A and 4B). Moreover, we compared the fecal samples using jackknifed UPGMA clustering based on weighted and unweighted UniFrac distances at the phylum level [30]. The clustering tree (Fig. 4C and 4D) indicated I/R altered gut bacterial flora. We then further analyzed the composition of the top 10 dominant phyla in pre- and post-I/R fecal samples. As shown in Fig. 5A, the relative abundance of the dominant phyla was similar and the top 4 most abundant phyla, namely Bacteroidetes, Firmicutes, Proteobacteria, and Spirochaetes, accounted for > 98% of the total identified phyla in both pre- and post-I/R groups. The percentages of Bacteroidetes in the pre- and post-I/R groups were 51.42% and 53.99%, respectively. The percentage of Firmicutes significantly decreased from 42.8–25.64% ($p = 0.026$), whereas that of Proteobacteria significantly increased from 2.8% in the pre-I/R surgery to 11.51% ($p = 0.017$) in post-I/R surgery. Similarly, the proportion of Spirochaetes in the post-I/R group (6.35 ± 5.93%) also increased by 5.49 times compared to pre-I/R group (1.16 ± 0.54%). Metastats analysis was utilized to further investigate the influence of I/R on the relative abundance of the

genera in fecal samples. The results showed that compared with pre-I/R group, I/R significantly decreased the relative abundance of Corynebacterium, Psychrobacter, Roseburia, Ruminococcus, and Paraprevotella, and significantly increased the relative abundance of Parabacteroides, Enterococcus, and Morganella (Fig. 5B).

We then compared the post-I/R surgery samples with the post-sham surgery samples to rule out surgical procedure itself on gut microbiota changes. A total of 157 unique OTUs were found in the post-I/R surgery samples, whereas 90 unique OTUs were found in the post-sham samples (Figure S3). The relative abundance of the phyla Bacteroidetes, Firmicutes, Proteobacteria, and Spirochaetes in both groups accounted for more than 98% of total number of phyla identified. The proportions of Bacteroidetes and Firmicutes were comparable in both post-sham and post-I/R groups. But when compared with pre-I/R surgery group, the relative abundances of Firmicutes in the post-sham (22.11 ± 2.2%) and post-I/R surgery (25.64 ± 2.54%) groups were much lower than those (42.8 ± 4.53%) in the pre-I/R surgery group. In contrast, the proportions of Proteobacteria in the post-sham (29.85 ± 11.09%) and post-I/R surgery (11.51 ± 2.12%) groups were higher than those abundance (2.8 ± 0.49%) in the pre-I/R surgery group, demonstrating that the proportion of Proteobacteria is positively associated, and the proportion of Firmicutes is negatively associated with surgical procedure itself. In addition, the proportion of Spirochaetes (6.35 ± 5.93%) in the post-I/R surgery was 2.5 times higher than those in the post-sham surgery (2.59 ± 2.31%) and pre-I/R surgery (1.16 ± 0.54%), which indicates that myocardial I/R injury regulates the relative abundance of Spirochaetes (Table.1).

At the genus level, the proportions of Escherichia, Parabacteroides, Streptococcus, Sutterella, Treponema, Paraprevotella and Ruminococcus between the post-sham and post-I/R surgery groups were undifferenced, while the proportions of Escherichia, Parabacteria, Streptococcus, Sutterella, and Treponema in both groups were higher than those in the pre-I/R surgery group, and the relative amount of Paraprevotella and Ruminococcus in both groups were lower than those in the pre-I/R surgery group, these results demonstrated that the surgery operation could influence the proportion of bacteria. However, I/R surgery could individually and significantly increase the relative abundance of Enterococcus in relative to those in the pre-I/R ($p = 0.008$) and post-sham group ($p = 0.02$), which was further revealed by metastats analysis (Table.2).

Open-chest surgical procedure also induces the change of gut microbiota composition in rat.

To directly analysis the potential effect of sham surgical procedure on the composition of intestinal flora, we compared the samples collected from rat pre- and post-sham operation. Figure 6 shows that at the phylum level, the percentages of Proteobacteria, one of the top 10 dominant phyla, were significantly increased from 1.38–29.85%, whereas those of Cyanobacteria and Tenericutes were significantly decreased from 0.97% and 1.23% to 0.02 and 0.21%, respectively, after sham surgery (Fig. 6A). At the genus level, Metastats analysis showed that the relative abundances of Escherichia, Bacteroides, Parabacteroides, Rc4–4, Bifidobacterium, SMB53, Bilophila, and Enterococcus were significantly increased, whereas those of Prevotella, Ruminococcus, Anaeroplasma, and Paraprevotella were

significantly decreased in the post-sham group (Fig. 6B). Taken together, these results indicate that open-chest sham surgical procedure can also alter the composition of gut microbiota.

Discussion

In this study, we employed a 16S rRNA amplicon deep sequencing method to evaluate I/R injury-induced changes of gut microbiota in rats. Our results showed that I/R altered the relative abundance of some unique bacteria population and these alterations might lead to inflammatory response in the heart after I/R. Since previous work suggested that stress may alter microbiota composition [31], we collected the fecal samples from sham and I/R group before and after surgery and compared their microbiota profile. Our data demonstrated that altherough distinct from each other, both myocardial I/R injury and open-chest surgery itself may change the proportion of gut bacteria.

The gut microbiota compositions changes caused by I/R were previously analyzed by quantitative polymerase chain reaction (PCR) or PCR-denaturing gradient gel electrophoresis (PCR-DGGE) [32]. However, the PCR-DGGE method displays various inherent errors and PCR bias [33], such as inaccurate abundance estimation or poor data reproducibility [34]. To address this problem, in current study, we utilized high-throughput sequencing technology targeting the V4 region of 16S rRNA gene to obtain a larger number of sequences in the fecal samples of rats subjected to myocardial I/R surgery and to identify the effects of I/R injury on bacterial taxa that are differentially expressed in rats subject to I/R.

Although alpha diversity analysis showed no difference among the pre-sham, post-sham, pre-I/R, and post-I/R samples, species richness among these samples significantly varied. The relative abundance of the phylum Proteobacteria was significantly higher in the post-sham and post-I/R samples than those in the pre-sham and pre-I/R groups (Table.1). The changes in gut microbiota compositions were consistent with the changes induced by other surgical interventions, such as Roux-en-Y gastric bypass (RYGB) [35–37]. Proteobacteria also dominates the altered gut microbial community during acute and chronic inflammation. The inflammatory response, one of factors in pathogenesis of myocardial I/R injury, possibly plays an important role in I/R injury. Thus, we speculate that the enrichment of Proteobacteria after surgery plays a role in driving inflammatory process in I/R injury. Although the Firmicutes/Bacteroidetes ratio was almost unchanged between the pre- and post-sham samples, the abundances of Firmicutes (22.11% ± 2.2%) and Bacteroidetes (44.95% ± 9.69%) were lower in post-sham samples than those in pre-sham samples (30.72% ± 6.55% and 64.01% ± 5.82%, respectively) (Table.1). In addition, compared with the abundances in pre-I/R surgery, the abundance of Firmicutes was significantly decreased, whereas that of Bacteroidetes was unaffected after I/R surgery (Table.1). This result is consistent with the results of fecal sample analysis of RYGB rats [38]. A healthy gut microbiota comprises two major phyla: Bacteroidetes and Firmicutes [39], and their abundances are related to inflammatory bowel disease (IBD). Decreased and increased abundances of Firmicutes and Bacteroidetes are respectively observed in IBD patients compared with controls [40]. Therefore, the altered abundances of Proteobacteria, Firmicutes and Bacteroidetes induced by myocardial I/R surgical operation may also be

an important factor mediating inflammatory response. The different degrees of changes might be partially attributable to altered pH, bile flow, and intestinal hormones induced by sham and I/R surgeries, and these factors in turn influenced the relative abundance of Proteobacteria, Firmicutes and Bacteroidetes [41].

Spirochaetes is the less prevalent bacteria distributed in the oral and intestinal microbiota, and it can cause periodontal diseases[42]. Demmer et. al., showed that the oral microbes may influence the cardiovascular system by direct invasion and induction of vascular injury or by releasing mediators such as endotoxins and lipopolysaccharide [43]. In the present work, phylum Spirochaetes was only increased in the post-I/R group (Table.1). Thus, we speculated that the Spirochaetes may play an important in promoting infiltration of macrophage into the heart, which is in consistent with finding that showed a direct response of macrophages to cardiac tissue invasion by Borrelia burgdorferi spirochetes [44].

At the genus level, Escherichia, Bacteroides, Parabacteroides, Paraprevotella, Ruminococcus, and Prevotella were dominant across all groups. Compared with preoperative levels, the relative abundances of Paraprevotella, Ruminococcus, and Prevotella were significantly decreased following sham or surgical procedure, whereas those of Escherichia, Bacteroides, and Parabacteroides were increased in post-sham or post-I/R groups (Fig. 6B and Table.2). Escherichia and Bacteroides, the two dominant genera enriched after sham surgery, are positively associated with low-grade inflammation and IBD in rats [45, 46]. The relative abundance of Ruminococcus, a member of the phylum Firmicutes, was significantly reduced by sham and I/R surgeries. Ruminococcus is necessary to help us digest resistant starches and is important for our digestive function [47], and Ruminococcus is negatively correlated with atherosclerotic events [25]. By contrast, the relative abundance of Parabacteroides, which belongs to the phylum Bacteroidetes, significantly increased after sham or I/R surgical procedure (Table.2). Studies have shown that Parabacteroides may inhibit inflammatory processes and tend to be missing in the gut of IBD patients [48]. In addition, the abundances of Prevotella and Paraprevotella, also members of the phylum Bacteroidetes, were significantly reduced by sham surgery, and they have been demonstrated to promote chronic inflammatory disease [49]. Therefore, the potential interactions among bacterial strains, rather than a specific organism, may play a role in the inflammatory responses in myocardial I/R.

According to the results of gut microbiota analysis, the effect of post-sham and post-I/R surgical procedures on the gut microbiota composition was quite similar, while the effect of post-I/R surgery on infiltration of macrophages was completely different from post-sham surgery (Fig. 2). It may be attributed to a lack of oxygen and glucose during ischemia, which causes mitochondrial respiratory dysfunction, metabolic exhaustion, and an increase in endothelium permeability. The intestinal permeability resulted in bacterial translocation into systemic circulation and led to the development of systemic inflammatory response and myocardial infarction [50]. However, this putative proinflammatory mechanism is yet to be identified and requires further investigation.

Methods

Rat model of I/R

Six-to-eight weeks old healthy male Sprague–Dawley rats (Certificate No. SCXK (Hunan) 2011–001) weighing ~400 grams were purchased from Hunan Silaike Jingda Experimental Animal Co., Ltd. The rats were maintained in environmentally controlled animal facility with a temperature of 25 ± 3 °C, relative humidity of 50% ± 10%, and 12/12 h light-dark cycle. Standard chow diet for rat were used, which contains moisture≤10%, protein≥18%, fat≥4%, fiber≤5%, calcium 1.0-1.8%, phosphorus 0.6-1.2 %, lysine≥8.2%, coarse ash≤8%, and methionine≥0.53%. After environmental adaptation for 7 days, the rats were randomized into two groups: sham group (n = 7) and myocardial I/R group (n = 11). All animal procedures were approved by the Institutional Animal Care and Use Committee of Jiangxi University of Traditional Chinese Medicine and conformed with the US National Institutes of Health's Guide for the Care and Use of Laboratory Animals.

The LAD coronary artery occlusion was performed as previously described [51]. Briefly, after induction of anesthesia with an intraperitoneal injection of chloral hydrate (10%, 3 mL/kg body weight), the rats were intubated and ventilated with a ventilator. The fourth intercostal space was accessed through a left thoracotomy. A 6-0 prolene suture was used to ligate (I/R group) or placed and removed (sham group) around the LAD coronary artery at the inferior edge of the left atrium with a piece of soft hose. Persistent ST segment elevation for 60 min was used as an assessment indicator of ischemia and monitored by PowerLab system (AD Instruments Shanghai Trading Co.). Then, the hose and slipknot were removed (reperfusion), and ST segment elevation was monitored. The thorax incision was then closed with a 4-0 nylon suture. The rats were allowed to recover for 48 h, during which time ST segment was monitored in the first hour after surgery.

Fecal sample collection

To examine whether I/R surgery influences gut microbiota composition, fecal samples from sham and I/R surgery groups were collected directly from the rectum of all animals before 1 h of ischemia and after 48 h of reperfusion, and the samples were stored in -80 °C for later DNA extraction.

Triphenyltetrazolium chloride (TTC) staining and infract analysis

Forty-eight hours after reperfusion, the hearts were excised and cut into four transverse slices from the apex to the ligation point. The heart slices were incubated in 1% Triphenyltetrazolium chloride (TTC) solution at 37 °C for 15 min, fixed with 10% formaldehyde solution for 24 h, and photographed with a digital camera on the next day. For each image, infarct area (white areas lacking TTC staining) and normal perfusion area (red areas) were measured with a planimeter and quantified by using the Image-Pro 6.0 software. For each slice, the infarct size was calculated by the ratio of white areas to the entire heart cross-section area, and the total infarct size was obtained by averaging the infarct size of the four slices.

Histological analysis and immunohistochemistry

Isolated hearts were fixed in 10% formaldehyde for over 24 h, sequentially dehydrated with an alcohol series, embedded in paraffin wax. The paraffin sections (5 μm) were stained with hematoxylin and eosin (H&E). Immunohistochemistry analysis was performed according to the procedures described by Hume and Gordon [52]. Briefly, 5 μm-thick sections were stained with anti-CD68 antibody (AbD Serotec, Raleigh, NC, USA, 1:100 dilution) against CD68, incubated with streptavidin-conjugated horseradish peroxidase, and colorimetrically detected with 3,3'-diaminobenzidine staining. Then, the sections were washed and incubated with hematin for 5 min to stain the nuclei. The positive areas were calculated from five random fields at 200× magnification.

DNA extraction and 16S rRNA gene sequencing

Total metagenomic DNA was extracted from fecal samples by using the CTAB method [53]. The DNA quality was assessed via agarose gel electrophoresis and spectrophotometry ($OD_{260/280}$). DNA concentration was determined with a Qubit fluorometer. Subsequently, the 16S rDNA V4 region was amplified using the universal primer 515F 5'-GTGCCAGCMGCCGCGGTAA-3' and 806R 5'-GGACTACHVGGGTWTCTAAT-3'. For the PCR product, the jagged ends of the DNA fragments were converted into blunt ends by using T4 DNA Polymerase, Klenow Fragment, and T4 Polynucleotide Kinase. Then, an “A” base was added to each 3' end to facilitate easier addition of adapters. Fusion primers with dual index and adapters were used for PCR, and fragments that were too short were removed using Ampure beads. In both cases, only the qualified library can be used for sequencing on an Illumina MiSeq PE250 (V2) platform, which generates paired-end reads. All new sequence data are available on NCBI BioProject (Accession nos.PRJNA602045).

Bioinformatics and statistical analyses

The overlapping paired-end reads were merged to tags by Fast Length Adjustment of Short reads v1.2.11 [54]. Filled tags were clustered into operational taxonomic units (OTUs) at 97% sequence similarity by using the scripts of USEARCH software (v7.0.1090) [55]. Taxonomic ranks were assigned to the OTU representative sequence using Ribosomal Database Project naïve Bayesian Classifier v.2.2 [56]. Alpha diversity was applied for analyzing the complexity of species diversity [57] in a sample by using several indices, including observed species, Chao1, ACE, and Shannon’s and Simpson’s indices. Beta diversity analysis was conducted using QIIME (v1.80) to evaluate differences of samples in terms of species complexity. Principal coordinate analysis (PCoA) was used to determine the differences between samples according to the matrix of beta diversity distance. Disparity in similarity among fecal samples in individual rats was calculated using a correlation matrix and was presented graphically in tree diagrams using an unweighted pair-group method with arithmetic mean (UPGMA) clustering.

Metastats (http://metastats.cbcb.umd.edu/) and R (v3.1.1) programs were used to determine which taxonomic groups were significantly different among the samples. The obtained *P* value was adjusted by Benjamini–Hochberg false discovery rate correction (function “p.adjust” in the stats package of R (v3.1.1)).

Declarations

Author contribution statement

Liang Qiu was responsible for conceiving, designing the study, supervising the study and revising the manuscript. Lingqin Su and Jun Yu wrote the manuscript. Cuifang Kuang performed the research. Manman Qin analyzed the data. All authors read and approved of the final manuscript.

Acknowledgement

This work was supported by grants (81570415, 81860090 and 31660328) from National Natural Science Foundation of China, Traditional Chinese Medicine Science and Technology Planning Project of Jiangxi Provincial Health and Family Planning Commission (2018B141), a program for the Key Laboratory for Pharmacology and Translational Research of Traditional Chinese Medicine of Nanchang (2018-NCZDSY-005), and Jiangxi University of Traditional Chinese Medicine First-class Discipline Construction-Chinese Medicine Project（JXSYLXK-ZHYAO021）JXSYLXK-ZHYAO107 and JXSYLXK-ZHYAO133）

Competing interests:

The authors declare that they have no conflict of interest.

Ethical approval:

All applicable international, national, and/or institutional guidelines for the care and use of animals were followed.

References

1. Lloyd-Jones D, Adams RJ, Brown TM, Carnethon M, Dai S, De Simone G, et al. Executive summary: heart disease and stroke statistics--2010 update: a report from the American Heart Association. Circulation 2010; 121:948-54.
2. Fleming SD, Tsokos GC. Complement, natural antibodies, autoantibodies and tissue injury. Autoimmun Rev 2006; 5:89-92.
3. Eltzschig HK, Eckle T. Ischemia and reperfusion--from mechanism to translation. Nat Med 2011; 17:1391-401.
4. Ettinger G, MacDonald K, Reid G, Burton JP. The influence of the human microbiome and probiotics on cardiovascular health. Gut Microbes 2014; 5:719-28.
5. Karlsson FH, Fak F, Nookaew I, Tremaroli V, Fagerberg B, Petranovic D, et al. Symptomatic atherosclerosis is associated with an altered gut metagenome. Nat Commun 2012; 3:1245.
6. Koeth RA, Wang ZE, Levison BS, Buffa JA, Org E, Sheehy BT, et al. Intestinal microbiota metabolism of L-carnitine, a nutrient in red meat, promotes atherosclerosis. Nature Medicine 2013; 19:576-85.

7. Sorkine P, Szold O, Halpern P, Gutman M, Greemland M, Rudick V, et al. Gut decontamination reduces bowel ischemia-induced lung injury in rats. Chest 1997; 112:491-5.
8. Souza DG, Vieira AT, Soares AC, Pinho V, Nicoli JR, Vieira LQ, et al. The essential role of the intestinal microbiota in facilitating acute inflammatory responses. J Immunol 2004; 173:4137-46.
9. Yoshiya K, Lapchak PH, Thai TH, Kannan L, Rani P, Dalle Lucca JJ, et al. Depletion of gut commensal bacteria attenuates intestinal ischemia/reperfusion injury. Am J Physiol Gastrointest Liver Physiol 2011; 301:G1020-30.
10. Emal D, Rampanelli E, Stroo I, Butter LM, Teske GJ, Claessen N, et al. Depletion of Gut Microbiota Protects against Renal Ischemia-Reperfusion Injury. J Am Soc Nephrol 2017; 28:1450-61.
11. Prakash A, Sundar SV, Zhu YG, Tran A, Lee JW, Lowell C, et al. Lung Ischemia-Reperfusion is a Sterile Inflammatory Process Influenced by Commensal Microbiota in Mice. Shock 2015; 44:272-9.
12. Sun J, Wang F, Ling Z, Yu X, Chen W, Li H, et al. *Clostridium butyricum* attenuates cerebral ischemia/reperfusion injury in diabetic mice via modulation of gut microbiota. Brain Res 2016; 1642:180-8.
13. Akira S, Uematsu S, Takeuchi O. Pathogen recognition and innate immunity. Cell 2006; 124:783-801.
14. Arumugam TV, Okun E, Tang SC, Thundyil J, Taylor SM, Woodruff TM. Toll-like receptors in ischemia-reperfusion injury. Shock 2009; 32:4-16.
15. Ha T, Liu L, Kelley J, Kao R, Williams D, Li C. Toll-like receptors: new players in myocardial ischemia/reperfusion injury. Antioxid Redox Signal 2011; 15:1875-93.
16. Kim E, Kim HC, Lee S, Ryu HG, Park YH, Kim JH, et al. Dexmedetomidine confers neuroprotection against transient global cerebral ischemia/reperfusion injury in rats by inhibiting inflammation through inactivation of the TLR-4/NF-kappaB pathway. Neurosci Lett 2017; 649:20-7.
17. Kilic U, Kilic E, Matter CM, Bassetti CL, Hermann DM. TLR-4 deficiency protects against focal cerebral ischemia and axotomy-induced neurodegeneration. Neurobiol Dis 2008; 31:33-40.
18. Paulus P, Rupprecht K, Baer P, Obermuller N, Penzkofer D, Reissig C, et al. The early activation of toll-like receptor (TLR)-3 initiates kidney injury after ischemia and reperfusion. PLoS One 2014; 9:e94366.
19. Li X, Yun Z, Tan Z, Li S, Wang D, Ma K, et al. The role of Toll-like receptor (TLR) 2 and 9 in renal ischemia and reperfusion injury. Urology 2013; 81:1379 e15-20.
20. Victoni T, Coelho FR, Soares AL, de Freitas A, Secher T, Guabiraba R, et al. Local and remote tissue injury upon intestinal ischemia and reperfusion depends on the TLR/MyD88 signaling pathway. Med Microbiol Immunol 2010; 199:35-42.
21. Perez-Chanona E, Muhlbauer M, Jobin C. The microbiota protects against ischemia/reperfusion-induced intestinal injury through nucleotide-binding oligomerization domain-containing protein 2 (NOD2) signaling. Am J Pathol 2014; 184:2965-75.
22. Chen LW, Chang WJ, Chen PH, Liu WC, Hsu CM. TLR ligand decreases mesenteric ischemia and reperfusion injury-induced gut damage through TNF-alpha signaling. Shock 2008; 30:563-70.

23. Frank A, Bonney M, Bonney S, Weitzel L, Koeppen M, Eckle T. Myocardial ischemia reperfusion injury: from basic science to clinical bedside. Semin Cardiothorac Vasc Anesth 2012; 16:123-32.
24. Wu ZX, Li SF, Chen H, Song JX, Gao YF, Zhang F, et al. The changes of gut microbiota after acute myocardial infarction in rats. PLoS One 2017; 12:e0180717.
25. Zhou X, Li J, Guo J, Geng B, Ji W, Zhao Q, et al. Gut-dependent microbial translocation induces inflammation and cardiovascular events after ST-elevation myocardial infarction. Microbiome 2018; 6:66.
26. Lam V, Su J, Hsu A, Gross GJ, Salzman NH, Baker JE. Intestinal Microbial Metabolites Are Linked to Severity of Myocardial Infarction in Rats. PLoS One 2016; 11:e0160840.
27. Lam V, Su J, Koprowski S, Hsu A, Tweddell JS, Rafiee P, et al. Intestinal microbiota determine severity of myocardial infarction in rats. Faseb Journal 2012; 26:1727-35.
28. Chen H, Zhang RQ, Wei XG, Ren XM, Gao XQ. Mechanism of TLR-4/NF-kappaB pathway in myocardial ischemia reperfusion injury of mouse. Asian Pac J Trop Med 2016; 9:503-7.
29. Kuntjoro I, Teo SG, Poh KK. Electrocardiography series. Non-ischaemic causes of ST segment elevation. Singapore Med J 2012; 53:367-70.
30. Lozupone C, Knight R. UniFrac: a new phylogenetic method for comparing microbial communities. Appl Environ Microbiol 2005; 71:8228-35.
31. Allen-Blevins CR, You X, Hinde K, Sela DA. Handling stress may confound murine gut microbiota studies. PeerJ 2017; 5:e2876.
32. Wang F, Li Q, Wang C, Tang C, Li J. Dynamic alteration of the colonic microbiota in intestinal ischemia-reperfusion injury. PLoS One 2012; 7:e42027.
33. Neilson JW, Jordan FL, Maier RM. Analysis of artifacts suggests DGGE should not be used for quantitative diversity analysis. J Microbiol Methods 2013; 92:256-63.
34. Bent SJ, Pierson JD, Forney LJ, Danovaro R, Luna GM, Dell'anno A, et al. Measuring species richness based on microbial community fingerprints: the emperor has no clothes. Appl Environ Microbiol 2007; 73:2399-401.
35. Liou AP, Paziuk M, Luevano JM, Jr., Machineni S, Turnbaugh PJ, Kaplan LM. Conserved shifts in the gut microbiota due to gastric bypass reduce host weight and adiposity. Sci Transl Med 2013; 5:178ra41.
36. Graessler J, Qin Y, Zhong H, Zhang J, Licinio J, Wong ML, et al. Metagenomic sequencing of the human gut microbiome before and after bariatric surgery in obese patients with type 2 diabetes: correlation with inflammatory and metabolic parameters. Pharmacogenomics J 2013; 13:514-22.
37. Zhang H, DiBaise JK, Zuccolo A, Kudrna D, Braidotti M, Yu Y, et al. Human gut microbiota in obesity and after gastric bypass. Proc Natl Acad Sci U S A 2009; 106:2365-70.
38. Li JV, Ashrafian H, Bueter M, Kinross J, Sands C, le Roux CW, et al. Metabolic surgery profoundly influences gut microbial-host metabolic cross-talk. Gut 2011; 60:1214-23.

39. Jandhyala SM, Talukdar R, Subramanyam C, Vuyyuru H, Sasikala M, Nageshwar Reddy D. Role of the normal gut microbiota. World J Gastroenterol 2015; 21:8787-803.
40. Walker AW, Sanderson JD, Churcher C, Parkes GC, Hudspith BN, Rayment N, et al. High-throughput clone library analysis of the mucosa-associated microbiota reveals dysbiosis and differences between inflamed and non-inflamed regions of the intestine in inflammatory bowel disease. BMC Microbiol 2011; 11:7.
41. Shin NR, Whon TW, Bae JW. *Proteobacteria*: microbial signature of dysbiosis in gut microbiota. Trends Biotechnol 2015; 33:496-503.
42. Visser MB, Ellen RP. New insights into the emerging role of oral *spirochaetes* in periodontal disease. Clinical Microbiology & Infection 2011; 17:502-12.
43. Demmer RT, Desvarieux M. Periodontal infections and cardiovascular disease: the heart of the matter. Journal of the American Dental Association 2006; 137:S14-S20.
44. Ruderman EM, Kerr JS, Telford SR, Spielman A, ., Glimcher LH, Gravallese EM. Early murine Lyme carditis has a macrophage predominance and is independent of major histocompatibility complex class II-CD4+ T cell interactions. Journal of Infectious Diseases 1995; 171:362-70.
45. Cani PD, Osto M, Geurts L, Everard A. Involvement of gut microbiota in the development of low-grade inflammation and type 2 diabetes associated with obesity. Gut Microbes 2012; 3:279-88.
46. Zhou Y, Zhi F. Lower Level of Bacteroides in the Gut Microbiota Is Associated with Inflammatory Bowel Disease: A Meta-Analysis. Biomed Res Int 2016; 2016:5828959.
47. Ze X, Duncan SH, Louis P, Flint HJ. Ruminococcus bromii is a keystone species for the degradation of resistant starch in the human colon. ISME J 2012; 6:1535-43.
48. Noor SO, Ridgway K, Scovell L, Kemsley EK, Lund EK, Jamieson C, et al. Ulcerative colitis and irritable bowel patients exhibit distinct abnormalities of the gut microbiota. BMC Gastroenterol 2010; 10:134.
49. Larsen JM. The immune response to Prevotella bacteria in chronic inflammatory disease. Immunology 2017; 151:363-74.
50. Yu L. Protective Mechanism against Gut Barrier Dysfunction in Mesenteric Ischemia/Reperfusion. Adaptive Medicine 2010; 2:11-22.
51. Vegh A, Komori S, Szekeres L, Parratt JR. Antiarrhythmic effects of preconditioning in anaesthetised dogs and rats. Cardiovasc Res 1992; 26:487-95.
52. Hume DA, Robinson AP, MacPherson GG, Gordon S. The mononuclear phagocyte system of the mouse defined by immunohistochemical localization of antigen F4/80. Relationship between macrophages, Langerhans cells, reticular cells, and dendritic cells in lymphoid and hematopoietic organs. J Exp Med 1983; 158:1522-36.
53. Ausubel FM, R. Brent, R. E. Kingston, D. D. Moore, J. A. Smith, J. G. Seidman, and K. Struhl. Preparation and analysis of DNA, p. 2.4.1–2.4.5. In F. M. Ausubel (ed.), Current protocols in molecular biology. John Wiley & Sons, Inc, New York, NY 1988.

54. Magoc T, Salzberg SL. FLASH: fast length adjustment of short reads to improve genome assemblies. Bioinformatics 2011; 27:2957-63.
55. Edgar RC. UPARSE: highly accurate OTU sequences from microbial amplicon reads. Nat Methods 2013; 10:996-8.
56. Fuller SJ, Burke IT, Mcmillan DGG, Ding W, Stewart DI. Population Changes in a Community of Alkaliphilic Iron-Reducing Bacteria Due to Changes in the Electron Acceptor: Implications for Bioremediation at Alkaline Cr(VI)-Contaminated Sites. Water Air & Soil Pollution 2015; 226:1-15.
57. Schloss PD, Westcott SL, Ryabin T, Hall JR, Hartmann M, Hollister EB, et al. Introducing mothur: open-source, platform-independent, community-supported software for describing and comparing microbial communities. Appl Environ Microbiol 2009; 75:7537-41.

Tables

Table 1
Relative abundance of significant difference of bacterial phylum among post-I/R, post-sham, pre-sham and pre-I/R

Phylum	pre-sham		post-sham		pre-I/R		post-/R	
	Mean (%)	SD	Mean (%)	SD	Mean (%)	SD	Mean (%)	SD
Proteobacteria	1.38	0.29	29.85[a]	11.09	2.80	0.49	11.51[b]	2.12
Firmicutes	30.72	6.55	22.11	2.20	42.80	4.53	25.64[b]	2.54
Bacteroidetes	64.01	5.82	44.95	9.69	51.42	4.21	53.99	7.22
Firmicutes/Bacteroidetes	0.48	1.13	0.49	0.23	0.83	1.08	0.47	0.35
Spirochetes	1.34	0.53	2.59	2.31	1.16	0.54	6.35	5.93

[a] $p < 0.05$ vs pre-sham, [b] $p < 0.05$ vs pre-IR,

Table 2
Relative abundance of significant difference of bacterial genus among post-I/R, post-sham and pre-I/R

Genus	pre-I/R		post-I/R		post-sham	
	Mean (%)	SD	Mean (%)	SD	Mean (%)	SD
Enterococcus	0.02	0.01	0.17	0.03	0.04[a]	0.00
Escherichia	0.06	0.01	2.33	2.04	25.06	10.32
Treponema	1.29	0.61	6.76	3.52	2.70	2.41
Parabacteroides	0.14 [b]	0.03	0.75	0.24	0.94	0.23
Streptococcus	0.01	0.01	0.36	0.27	0.61	0.38
Sutterella	0.43	0.32	2.50	1.34	1.87	1.00
Ruminococcus	2.63 [b]	0.47	0.70	0.26	0.66	0.33
Paraprevotella	5.44 [b]	2.05	0.87	0.18	0.45	0.14
[a] $p < 0.05$ vs post-IR, [b] $p < 0.05$ vs post-IR, [c] $p < 0.01$ vs post-IR						

Figures

Figure 1

Model of myocardial I/R injury. (A) Time courses of ST segment continuously recorded throughout the experiment (0–60 min: ischemia, 60–120 min: reperfusion). (B) Representative images of TTC-stained heart sections. (C) Infarct size in sham (n = 7) and I/R group (n = 11) subjected to ischemia (60 min) and followed by 48 h of reperfusion. Data are expressed as mean ± S.E.M. P < 0.05, P < 0.001 compared to sham group.

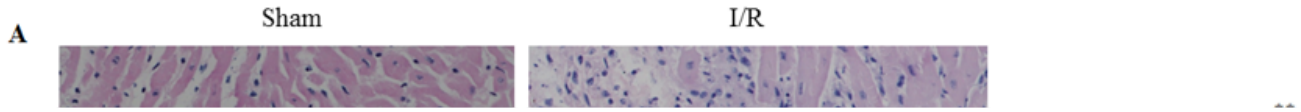


Figure 2

The effects of myocardial I/R on tissue inflammation. (A) Hearts were retrieved after reperfusion and subjected to H&E and CD68 immunohistochemical staining. Representative images of macrophages with H&E and immunohistochemical staining are shown. (B) Inflammation score of H&E stain was determined, and significant differences in CD68-positive cells between the I/R group (n = 11) and sham group were determined (n = 7). Values are the mean ± S.E.M. of three independent experiments. ▯▯P < 0.01 compared to sham group.

Figure 3

Alpha diversity indices of the bacterial communities. The richness of gut microbiota in the sham and I/R groups was evaluated based on observed species and Chao1 and ACE indices; the diversity of gut microbiota in the sham group (n = 3) and I/R group (n = 3) was estimated using Shannon's and Simpson's indices. Except for the Simpson's index, the other indices showed no significant difference between the sham and I/R groups. ▯P < 0.01 compared to sham group.

Figure 4

Difference in microbial diversity of post- and pre-I/R surgery samples. Principal coordinate analysis (PCoA) of the samples with unweighted UniFrac (A) and weighted UniFrac (B) distances showed the distinct cecal microbial composition between the pre- and post-I/R groups. Each data point represents a cecal sample, and percent variation explained by PCs is indicated on the axes. The hierarchical clustering tree structure of UPGMA based on unweighted UniFrac (C) and weighted UniFrac distances (D) further revealed the differences between the study groups.

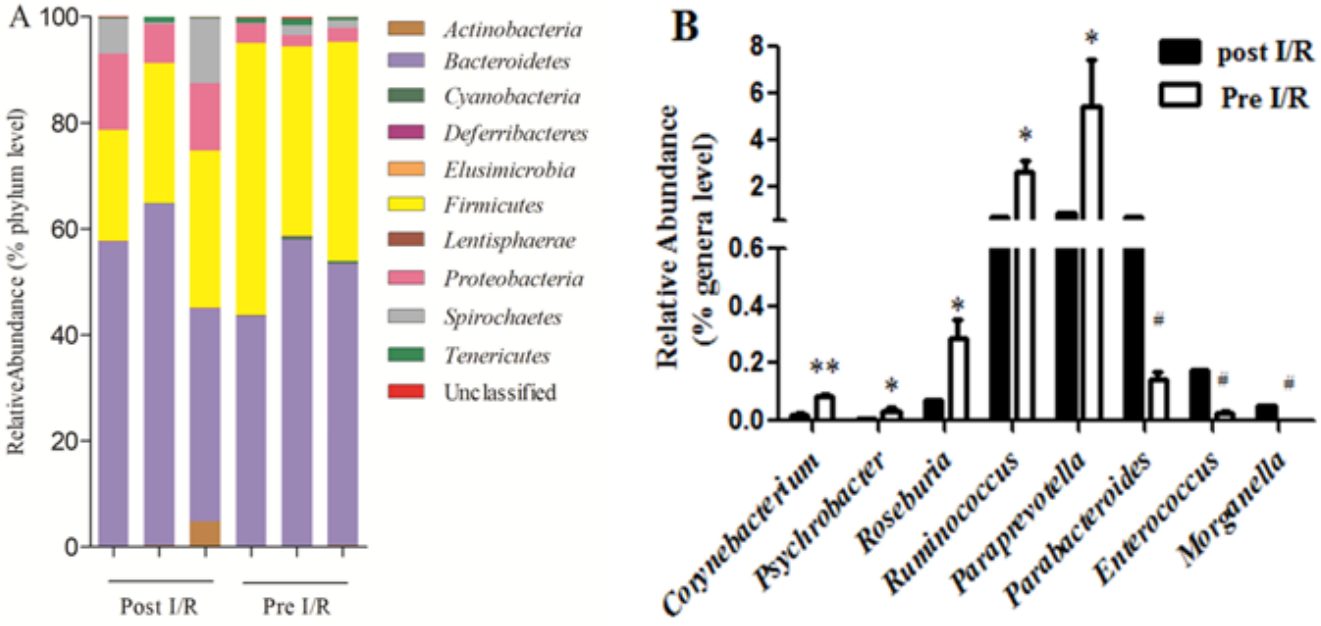


Figure 5

Comparison of relative proportions of gut microbiota between pre- and post- I/R surgery. (A) Relative abundance of the dominant bacteria at the phylum level. (B) Significant difference of relative abundances between pre- and post-I/R surgery at the genus level. *P < 0.05, **P < 0.01 compared to post I/R surgery; #P < 0.05, ##P < 0.01 compared to post I/R surgery.

Figure 6

Comparison of relative proportions of gut microbiota in the pre- and post-sham surgery samples. (A) Relative abundance of the dominant bacteria at the phylum level. (B) Significant difference of the relative abundances between pre- and post-sham surgery samples at the genus level. *P < 0.05, **P < 0.01 compared to post sham samples; #P < 0.05; ##P < 0.01 compared to post sham samples.

Supplementary Files

This is a list of supplementary files associated with this preprint. Click to download.

- supplementalfile.docx